Journal of Controlled Release 381 (2025) 113600

Contents lists available at ScienceDirect

Journal of Controlled Release

journal homepage: www.elsevier.com/locate/jconrel

AAV9-delivery of *interleukin-37b* gene prevents recurrent herpetic stromal keratitis *via* the SIGIRR pathway in mice

Jing Wu [a,g,1], Ye Liu [b,g,1], Chenchen Wang [c,g,1], Yurong Cai [d], Xiaomin Zhu [e], Ruining Lyu [g], Qiao You [g], Xiaoqian Liu [f], Qin Qin [h,*], Yajie Qian [i,*], Deyan Chen [f,g,*]

[a] *Department of Preventive Medicine, School of Public Health, Fujian Medical University, Fuzhou, China*
[b] *Department of Ophthalmology, Tianjin First Central Hospital, Tianjin, China*
[c] *The Eye Hospital of Wenzhou Medical University, Wenzhou Medical University, Hangzhou, China*
[d] *Ningxia Institute of Clinical Medicine, Central Laboratory,People's Hospital of Ningxia Hui Autonomous Region, Ningxia Medical University, Yinchuan, China*
[e] *Department of Ophthalmology, Affiliated Jinling Hospital, Medical School of Nanjing University, Nanjing, China*
[f] *Eye-X Institute, Bengbu Medical University, Bengbu, China*
[g] *Medical school of Nanjing University, Nanjing, China*
[h] *Department of Ophthalmology, Nanjing Drum Tower Hospital, The Affiliated Hospital of Nanjing University Medical School, Nanjing, China*
[i] *Department of Cariology and Endodontics, Nanjing Stomatological Hospital, Medical School of Nanjing University, Nanjing, China*

A R T I C L E I N F O

Keywords:
Interleukin-37b
Recurrent herpetic stromal keratitis
SIGIRR
HSV-1 infection

A B S T R A C T

Ocular herpes simplex virus type I (HSV-1) infection can lead to herpes stromal keratitis (HSK), a condition that may recur throughout a person's life and often results in progressive corneal scarring, which ultimately causes visual impairment. Since existing antiviral agents are ineffective against recurrent HSK, we aimed to explore a strategy to prevent or control recurrent HSK. Adeno-associated virus (AAV) delivery system can transduce target genes into corneal epithelial cells and establish long-term stable gene expression, and providing a promising approach for the prevention and management of recurrent HSK. In this study, interleukin-37 (IL-37), an anti-inflammatory factor, is identified as a therapeutic agent for recurrent HSK *via* the SIGIRR pathway. AAV9-IL-37bΔ1–45 gene therapy prevents recurrent HSK in HSV-1 latently infected mice and alleviates corneal injury in mice with HSK. In conclusion, our present study establishes a strong foundation for the prevention of recurrent HSK through AAV9-IL-37bΔ1–45 gene therapy.

1. Introduction

Herpes simplex virus (HSV) is one of the most prevalent human viruses globally [1]. HSV-1, a key member of the *Herpesviridae* family, primarily infects the skin, lips, tongue, and oral mucosa, resulting in the formation of watery blisters. Following initial lytic replication in epithelial cells, HSV-1 establishes lifelong latency in neurons located within the trigeminal ganglion [2]. Latent HSV-1 can be reactivated when the host is immunocompromised [3]. The reactivated HSV-1 can travel to the innervated mucosal epithelial surface to resume lytic replication. For instance, reactivation of HSV-1 can lead to anterograde transport to corneal tissues, resulting to recurrent herpetic stromal keratitis (HSK), which can cause permanent blindness in severe, untreated cases [4,5]. Unfortunately, there is an absence of vaccines to inhibit latent and recurrent HSV-1 infections, presenting a formidable challenge in the prevention and management of vision loss associated with recurrent HSK. Acyclovir (ACV) is widely recognized as the primary therapeutic agent for HSK; however, it remains insufficient in addressing the ongoing issue of recurrent HSK episodes [6,7]. Developing more effective therapies is crucial for HSK patients worldwide. We have previously established a mouse model for HSK and utilized it to evaluate the antiviral activity of several antiviral agents [2,8]. Here, we aimed to continue exploring effective prevention and treatment strategies for recurrent HSK.

Interleukin-37 (IL-37) is a recently identified member of the IL-1 family, functioning as a novel anti-inflammatory cytokine [9]. IL-37 exists in five different isoforms (IL-37a–e), with IL-37b being the largest and the predominant form found in peripheral blood [10]. IL-37b

* Corresponding authors at: Medical School of Nanjing University, 22# Hankou Road, Nanjing 210093, Jiangsu Province, China.
E-mail addresses: qinqin.1219@hotmail.com (Q. Qin), qian_qq@163.com (Y. Qian), chendeyan@nju.edu.cn (D. Chen).
[1] These authors have contributed equally to this work.

https://doi.org/10.1016/j.jconrel.2025.113600
Received 26 November 2024; Received in revised form 11 February 2025; Accepted 1 March 2025
Available online 3 March 2025

binds to the IL-18 receptor alpha (IL-18Rα), subsequently triggering an anti-inflammatory response through the activation of IL-1R8 (SIGIRR) [11]. Previous studies have indicated that the IL-37/SIGIRR axis not only suppresses inflammation associated with HIV infection but also inhibits viral replication [12]. This suggests that the IL-37/SIGIRR pathway plays a crucial role in the host's defense against viral infections. Investigating the potential therapeutic role of the IL-37/SIGIRR pathway in recurrent HSK is intriguing.

Delivering biological agents within the corneal tissue has been posing a significant challenge [13]. Adeno-associated virus (AAV) has emerged as a highly effective gene therapy vector, demonstrating efficacy in treating various ophthalmic diseases [14]. AAV9 has been recognized as an efficient delivery method for the long-term transduction of target genes into the corneal endothelium, showing safety and good tolerability during glaucoma treatment [15]. Although mice lack the homologous *Il-37* gene [16], IL-37 receptors such as IL-18Rα and SIGIRR are present in the corneal tissues of C57BL/6 J and BALB/c mice, allowing them to effectively pass the signals in response to human IL-37 protein treatment [17,18]. This capability is also demonstrated in IL-37 transgenic mice, which exhibit characteristics similar to human colorectal cancer through the IL-37/SIGIRR pathway [19]. Above evidence enables the evaluation of the therapeutic effect of AAV9-delivered *IL-37b* gene in the corneas of mice following HSV-1 infection.

In this study, given the significant reduction of IL-37 levels in the corneal tissues of HSK patients, we focused on the preventive and therapeutic roles of IL-37 in a mouse model of recurrent HSK. We successfully established stable gene expression of Il-37bΔ1–45 in mouse corneal tissue for at least four weeks using the AAV9 delivery system. Furthermore, we assessed the preventive effects of AAV9-delivered Il-37bΔ1–45 on recurrent HSK and confirmed the anti-HSK effects of IL-37b through the SIGIRR pathway. This research may provide a novel therapeutic approach for recurrent HSK, owing to the long-lasting efficacy of the AAV9 transduction system.

2. Materials and methods

2.1. Recombinant protein

Recombinant human IL-37b protein (rhIL-37b), which contains amino acids Val 46 to Asp 218 (Accession # AAH20637.1), was purchased from ACRO-Biosystems group. The protein was dissolved in PBS buffer to achieve a final concentration of 100 μg/μL. Fluorescein sodium was purchased from MACKLIN (Cat#: F809553-25 g).

2.2. Construction and production of the AAV9 vector

The AAV vector plasmid GV629, which contains the elements AAV-pTIE-EGFP-MCS-SV40 polyA (purchased from Shanghai Genechem Co., Ltd.), was used in this study. TIE (165–1458) is a mouse endothelial cell-specific promoter that initiates the expression of the human Il-37bΔ1–45 gene in mouse cells. EGFP, a fluorescent protein, facilitates the observation of AAV9 transduction efficiency. The MCS is a short DNA sequence containing up to 20 restriction enzyme sites, which serve as insertion sites for exogenous genes. Among these, the *Nhe*I and *Xho*I sites were utilized in this study. SV40 polyA acts as a transcription termination signal. The map information for the GV629 is provided in the Supplementary Materials. The AAV9-control is an empty vector based on GV629 (AAV9-vector). The AAV9-IL-37b is the GV629 vector packaged with the human *Il-37bΔ1–45* gene (Accession#AAH20637.1), which spans from Val46 to Asp218 (AAH20637.1(46-218aa)-3 × Flag).

The following primers were utilized for the amplification of the *Il-37b* gene: forward: 5'-ACGAGCTGTACAAGGCTAGCATGGTGCACACTAGCCCTAAG-3′; reverse: 5'-GCTATCATATGTTACTCGAGTCATTTGTCGTCATCATCCTTATAG-3′. The vector and the human *Il-37b* gene sequence were digested with the restriction enzymes *Nhe*I and *Xho*I, and complete cloning was achieved *via* the In-Fusion recombination method. The recombinant vector was verified by DNA sequencing. The details of the Il-37b (AAH20637.1(46-218aa)-3 × Flag) gene sequence construction is provided in the Supplementary Materials.

The plasmids, including IL-37b-flag or empty vectors, were transfected into HEK-293 T cells using Lipofectamine 2000 (Invitrogen; Cat#: 11668019), along with the AAV backbone packaging plasmids pHelper and pRepCap. AAV was harvested 72 h after transfection, and AAV9 was purified through iodixanol gradient ultracentrifugation and subsequently concentrated. The purified AAV viruses were titered using a quantitative PCR-based method. All AAV viruses used in this study were prepared in a 0.001 % Pluronic F-68 solution (Poloxamer 188 Solution, PFL01–100 mL,Caisson Laboratories, Smithfield, UT, USA). Finally, AAV9-Vector and AAV9-IL-37bΔ1–45 with storage titers of 1.0×10^{13} v.g./mL and 2.03×10^{13} v.g./mL were obtained, respectively. The packaged virus is supplemented with 5 % glycerol and stored at −80 °C.

The titers of AAV9 were determined by quantifying the genome copy numbers *via* using a PCR assay with ABI SYBR Green Master Mix (Life Technologies). A standard curve was established using a plasmid as the standard, and the titer of the sample to be tested was obtained by comparing it to the standard curve. A 20 μL reaction system was employed in this experiment, which included 10 μL of 2 × SYBR Green Mix, 0.5 μL of forward primer, 0.5 μL of reverse primer, 4 μL of ddH2O, and 5 μL of DNA samples. The ABI Prism 7500 Sequence Detection System was used to obtain the Ct value, following the thermal cycling conditions of 95 °C for 10 min, 95 °C for 15 s, and 60 °C for 35 s, for a total of 40 cycles. After obtaining the Ct value, the sample concentration was calculated from the standard curve drawn from the Ct value of the standard. The final value of the sample concentration was obtained by dividing the assay value by the dilution and multiplying by 2. The reason for the multiplication by 2 is that the standard is double-stranded while the AAV is a single-stranded linear DNA-deficient virus. The primers listed below were utilized for the detection of the AAV9 genome: forward: 5′- AAGATTCAAAGTGCGCTGCTGGTG-3′, reverse: 5′-TTGCCTGATACCTGGCAGATGGAA-3′.

2.3. Cell lines

The human SV40 immortalized corneal epithelial cell line (HCEC) was obtained from Hunan Fenghui Biotechnology Co.,Ltd. (Hunan, China) and cultured in Dulbecco's modified Eagle's Medium DMEM (Thermo Fisher Scientific), supplemented with 10 % fetal bovine serum (FBS, ExCell Bio, Shanghai). Vero cells, HeLa cells, and mouse embryonic fibroblasts (MEF) cells were acquired from ATCC, and were maintained in DMEM containing 10 % FBS in a 37 °C humidified atmosphere with 5 % CO_2.

2.4. Viruses

The HSV-1F strain, utilized in both *in vivo* and *in vitro* assays, was generously provided by Prof. Peng Tao from the Guangdong South China United Vaccine Institute of Guangzhou Medical University. The HSV-1F/GFP strain, which is derived from the HSV-1F strain, contains an enhanced green fluorescent protein (eGFP) gene, and was kindly donated by Prof. Erguang Li at Medical School of Nanjing University. Both HSV-1F and HSV-1F/GFP strains were propagated on Vero cells following a standard protocol as previously described [8]. Viral proteins, including glycoprotein D1 (gD-1) and infected-cell polypeptide 4 (ICP4), are critical for HSV-1 infections and are commonly employed to quantitatively assess viral replication.

2.5. Assessment of antiviral activity

HCEC cells were infected with the HSV-1F strain (MOI = 1) in the presence of rhIL-37b or acyclovir (ACV). Subsequently, a quantitative polymerase chain reaction (qPCR) assay was employed to determine the percentage of viral inhibition by measuring the mRNA expression of *gd-*

1. The half-maximal inhibitory concentration (IC_{50}) was calculated from dose-response curves using GraphPad Prism software. The Cell Counting Kit 8 assay was conducted to determine the 50 % cytotoxic concentration (CC_{50}) of rhIL-37 or ACV *in vitro*, with the data analyzed using GraphPad Prism. The selectivity index (SI) was defined as the ratio of the safe concentration range for assessing drug effects, calculated using the formula $SI = CC_{50}/IC_{50}$.

2.6. Antibodies

Antibodies specific for IL-37, ICP4, gD-1, SIGIRR, IL-18Ra, and GAPDH were shown in the Table 1.

2.7. RNA extraction, reverse transcription, and qRT-PCR analysis

Total RNA was extracted using TRIzol reagent (Life Technologies) and reverse transcribed using the PrimeScript RT Master Mix for RT-PCR (TaKaRa). Quantitative real-time PCR (RT-qPCR) was performed with the ABI SYBR Green Master Mix (Life Technologies) on an ABI Prism 7500 Sequence Detection System. GAPDH was served as the reference gene for normalizing mRNA levels, including the quantification of mRNA, including HSV-1 viral RNA. All reactions were performed in triplicate, and data analysis was conducted using the $2^{-\Delta\Delta Ct}$ method. The sequences of the real-time PCR primer pairs are presented in Table 2 below:

2.8. Western blotting

To prepare whole-cell lysates, cells were lysed in RIPA lysis buffer (Invitrogen) supplemented with a protease inhibitor cocktail (Thermo Fisher) for 30 min on ice, followed by centrifugation at 12,000 rpm for 15 min. The protein concentration of the cell lysates was measured using a BCA protein assay kit (Thermo Fisher). Next, cell extracts were separated using 10 % SDS-PAGE. The protein concentration was determined with the Bradford assay. Following electrophoresis, proteins were transferred to PVDF membranes (Millipore). The membranes were blocked for 1 h at room temperature in 2 % BSA. They were then probed overnight at 4 °C with primary antibodies specific for IL-37, ICP4, gD-1, IL-18Rα, SIGIRR, and GAPDH at appropriate dilutions. Subsequently, the membranes were incubated with secondary antibodies for 1 h at room temperature. Finally, band intensities were quantified using ImageJ software from the National Institutes of Health.

2.9. Ethics statement and establishmentof mouse model

Male BALB/c mice, C57BL/6 J mice, and *Sigirr*$^{-/-}$ mice at 6-week-old were housed under pathogen-free conditions. Specific pathogen-free (SPF) BALB/c and C57BL/6 J mice were obtained from Yangzhou University Center for Comparative Medicine (Yangzhou, China) and Charles River Laboratories (Pinghu, China). *Sigirr*$^{-/-}$ mice were a gift from Prof. Damo Xu (Shenzhen University, Shenzhen, China) [20]. All animal experimental procedures were approved by the Committee on the Use of Live Animals by the Ethics Committee of Nanjing First Hospital of Nanjing Medical University, Nanjing, Jiangsu Province, China (DWSY-28257). This study adheres to the Association for Research in Vision & Ophthalmology (ARVO) Statement for the use of animals in the Research of Ophthalmic and Vision.

The HSV-1 corneal infection mouse model was established based on a previous published study with modifications [21]. Briefly, mice were anesthetized, and the right cornea was scratched in a '#' shape using a 33-gauge needle under a dissection microscope. Next, a 10 μL drop of HSV-1F strain (1.2×10^6 PFU) strain stock solution was applied to the scratched eye. For the recurrent HSK model, 6-week-old BALB/c male mice were initially inoculated in the right eye with 1×10^5 PFU of HSV-1F strain, which is consistent with the acute HSV-1 corneal infection model. At one day post-infection (dpi), the mice were treated with 1 mL of pooled human serum (Sigma, Temecula, CA, USA), which exhibits anti-HSV reactivity with a 50 % viral neutralization effective dose of 1:800, to protect them from HSK during the initial infection. The surviving mice after the acute infection were maintained for 35 dpi. The right eyes of the mice were exposed to 302 nm ultraviolet radiation B (UV-B) light for 3 min. Levofloxacin eye drops were administered once daily to control bacterial infection, starting 5 h post-infection. Corneal morphology was assessed by capturing corneal images of the cornea using a stereomicroscope. The condition of the injured cornea was evaluated under a microscope using cobalt blue light with a wavelength of 460 nm. The severity of the disease was assessed using the HSK disease score and the fluorescein sodium staining score. HSK disease scoring (0–5) was conducted in a blinded fashion based on the previously reported criteria [21], as detailed in Table 3. More detailed images in supplementary document to explain the different grades of HSK disease (0–5 points) (**Fig. S1**). Then, 20 μL of 0.1 % fluorescein sodium pohthalmic solution was dropped into the right eye of mice, and the solution was gently aspirated with a cotton swab. The injured cornea was photographed under the microscope with cobalt blue light at a wavelength of 460 nm. The severity of the disease was measured using the HSK disease score and fluorescein sodium staining score, respectively. The fluorescein staining score was graded from 0 (none) to 12 (most severe) according to a previous study [22], as listed in Table 4.

Additionally, body weights and eye swabs were collected from the mice at 1, 3, and 5 dpi. The eye swabs were immediately stored at −80 °C for virus titration. For histopathological analysis, the right eyes of the mice were removed at 6 dpi, fixed, embedded, sectioned, and stained. The sections were stained with hematoxylin and eosin (H&E), and subsequently imaged using a 20 × objective lens with an OLYMPUS IX73 microscope.

2.10. rhIL-37b and gene therapy using AAV9-Il-37bΔ1–45 in the establishment of a mouse model

To explore the preventive and therapeutic effects of AAV9-IL-37bΔ1–45 and rhIL-37b respectively in the HSV-1 corneal infection mouse model and the recurrent HSK mouse model, we established the treatment models for rhIL-37b and AAV9-IL-37bΔ1–45 separately. HSV-1 corneal infection mice were administered 10 μL of rhIL-37b (1.0 μg/mouse) *via* subconjunctival injection at 1, 3, 5 dpi. In the recurrent HSK mice model, mice were administered 10 μL of rhIL-37b (1.0 μg/mouse) *via* subconjunctival injection at 36, 38, 40 dpi following UV-B-induced reactivation.

In the HSV-1 corneal infection model, mice were administered 1.0×10^{11} v.g. of either AAV9-Vector or AAV9-IL-37bΔ1–45 in a 10 μL volume *via* subconjunctival injection prior to HSV-1 inoculation. Subsequently, these mice were continued to be utilized to establish a model of HSV-1 corneal infection. In the recurrent HSK model, HSV-1 corneal-infected mice surviving 7 days post-HSV-1 infection were administered 10 μL either of 1.0×10^{11} v.g. AAV9-Vector or 1.0×10^{11} v.g. AAV9-IL-37bΔ1–45 *via* subconjunctival injection. After 3 weeks, the right eyes of

Table 1
Details of antibodies used in this project.

Product name	Company	Product Number	Dilutions (WB)	Dilutions (IF)
Anti-IL-37	Fine Biotech	FNab04275	1:1000	1:100
Anti-ICP4	Santa Cruz	SC-69809 Lot#J1520	1:500	1:100
Anti-gD-1	Santa Cruz	SC-69802 Lot#L3014	1:500	1:100
Anti-GAPDH	ProteinTech	60,004–1-1 g	1:2000	N/A
Anti-SIGIRR	ProteinTech	27,828–1-AP	1:1000	1:100
Anti-IL-18Rα	R&D	MAB840	1:1000	1:100

Table 2
Sequence of primers.

	Forward (5′-3′)	Reverse (5′-3′)
gD-1	AGCAGGGGTTAGGGAGTTG	CCATCTTGAGAGAGGCATC
ICP4	GGCCTGCTTCCGGATCTC	GGTGATGAAGGAGCTGCTGTT
IL-37b human	CCCAGTGCTGCTTAGAAGAC	TGAGATTCCCAGAGTCCAG
IL-6 mouse	TACCACTTCACAAGTCGGAGGC	CTGCAAGTGCATCATCGTTGTTC
IL-17E mouse	TGGCTGAAGTGGAGCTCTGCAT	CCCGATTCAAGTCCCTGTCCAA
CXCL2 mouse	CATCCAGAGCTTGAGTGTGACG	GGCTTCAGGGTCAAGGCAAACT
CCL2 mouse	GCTACAAGAGGATCACCAGCAG	GTCTGGACCCATTCCTTCTTGG
GAPDH human	GAGTCAACGGATTTGGTCGT	CTTGATTTTGGAGGGATCTCGC
GAPDH mouse	CCATCAACGACCCCTTCATTGACC	TGGTTCACACCCATCACAAACATG
SIGIRR human	CCTCCTTCACTCTTCAGAGAGC	ACGGCACTTGACATAGAGCAGG
SIGIRR mouse	CAGTGGCTGAAAGATGGTCTGG	AGTTGAGCACCAGGACACTGGA
IL-18Rα human	GGAGGCACAGACACCAAAAGCT	AGGCACACTACTGCCACCAAGA
IL-18Rα mouse	AGAGCTGATCCAGGACACATGG	TGGTGGACAGAAAACACGCAGG

Table 3
The HSK disease score.

Corneal epithelial score
0 Entire epithelial lesion
1 Diffuse punctate lesion
2 Dendritic lesions occupying less than 1/4 of the entire epithelial area
3 Severe dendritic lesions extending more than 1/4 of the entire epithelial area
4 Geographic lesions on the epithelial area
5 Eye completely swollen shut

Table 4
The fluorescein staining score.

Fluorescein staining score (divided into four quadrants, with 0–3 points per quadrant)
0 No corneal coloration
1 Corneal punctate staining
2 Corneal dendritic lesions
3 Corneal Geographic lesions

these mice were exposed to UV-B light at 35 dpi to induce recurrent HSK.

2.11. Viral titer determination

Ocular swabs samples were collected from the right eyes of infected mice from 1 dpi to 5 dpi using a cotton applicator. Each swab was placed in 1 mL of tissue culture medium and stored at −80 °C until use. The viral titers were determined using a standard plaque assay with Vero cells as previously reported [8].

2.12. Immunofluorescence assay

Dewaxed eye tissue sections were fixed in 4 % paraformaldehyde for 15 min and then permeabilized with 0.5 % Triton X-100 for an additional 15 min. Following this, the sections were incubated in a 1 % BSA blocking buffer for 1 h at room temperature. They were subsequently stained with primary and secondary antibodies, while the cell nuclei were labeled with DAPI. Images were captured using an panoramic tissue section imaging system (PanoBrain, Meca Scientific, PB-ST100).

2.13. H&E staining

The eyes and spleens were perfused with 4 % paraformaldehyde (PFA) and subsequently embedded in paraffin. Sections with a thickness of 4 μm were prepared and stained with hematoxylin and eosin.

2.14. Histopathology of the spleen

The splenic index was defined as the ratio of spleen weight to body weight (mg/g). Spleen pathology was assessed based on the degree of decreased cellularity in the red pulp, as outlined in a previous study [23]. The severity of the pathology was categorized into five grades: Grade 1 indicated complete depletion of red pulp (RP) in the observed field; Grade 2 indicated the absence of lymphocyte islands, although scattered lymphocytes remained visible; Grade 3 indicated a significant reduction in both the number and size of lymphocyte islands; Grade 4 indicated a slight reduction in the number and size of lymphocyte islands; Grade 5 indicated a normal number and size of lymphocyte islands.

2.15. Lentivirus-mediated knockdown of IL-18Rα or SIGIRR using shRNA

To generate IL-18Rα or SIGIRR-knock-down cells, we utilized pLKO.1-puro-based lentiviruses that expressing specific short hairpin RNAs (shRNA) targeting IL-18Rα or SIGIRR. HeLa cells were infected with lentiviruses expressing shRNAs against IL-18Rα, SIGIRR, or a control vector (pLKO). The infected cells were subsequently selected with puromycin to establish stable IL-18Rα knockdown, SIGIRR knockdown, or control (shNC) pLKO cells. The efficiency of the knockdown was confirmed by qRT-PCR analysis and was used for subsequent experiments to evaluate the expression of target proteins. The shRNA sequences targeting human SIGIRR or IL-18Ra are listed in Table 5.

2.16. Human clinical samples

This study was approved by the Ethics Committee of Jiling Hospital, Medical School of Nanjing University, Nanjing, China (2022DZGZR-091). All patients provided an informed consent form prior to enrollment. This study adheres to the principles oulined in the Declaration of Helsinki. Ocular swabs and blood samples were collected from patients with HSK as well as from healthy individuals without HSV-1 infection who underwent unrelated corneal surgery.

2.17. Statistical analysis

Statistical analysis was conducted using GraphPad Prisms 6.0 software. Results are presented as means ± SEM, based on at least three biological replicates. The normality of the data was initially assessed using the *Shapro-Wiik* test. For data that conformed to a normal distribution, comparisons between two groups were analyzed using two-tailed *Student's t*-test or a *paired t*-test. *One-way ANOVA* or *repeated measures ANOVA,* followed by *Dunnett-t*-test were employed to compare more than two groups, provided that *F*-test indicated $P > 0.05$ and there

Table 5
Sequence of shRNA.

Gene name	Target sequences
Sigirr human	CCTCCTTCACTCTTCAGAGAGC
Il-18Rα human	TCAGAGCTTTGTCACTTGCCA

was no significant variance in homogeneity. Nonparametric tests were applied to sets that did not conform to a normal distribution or with for which the *F*-test $P < 0.05$: *Kruskal-Wallis H* test was used to compare more than two data groups. *Wilcoxon* test was used to compare the repeated measures data of the two groups or the two independent samples.

3. Results

3.1. IL-37 levels were decreased in both ocular swabs and serum of HSK patients

To investigate the levels of IL-37 in patients with HSK, we collected early morning fasting venous blood samples and ocular swabs from theses HSK patients (Fig. 1A). Compared to healthy individuals, the IL-37 protein levels of IL-37 were significantly reduced in both the ocular swabs and serum of HSK patients (Fig. 1B). *In vitro*, IL-37 mRNA and protein expression were also reduced in HSV-1-infected HCEC cells, a cell line commonly used to study corneal lesions (Fig. 1C-D). This suggests that the down-regulation of IL-37 induced by HSV-1 infection may contribute to the development of HSK. The progression of HSK is associated with the lytic replication of HSV-1 within corneal tissues. We further explores the potential role of IL-37 supplementation in both HSV-1 replication and the management of HSK.

3.2. IL-37bΔ1–45, but not IL-37bΔ1–20, inhibits HSV-1 replication in vitro

The precursor of IL-37b can be cleaved in the cytosol to produce two forms of mature IL-37b: a short form, IL-37b (IL-37bΔ1–20), and a long form, IL-37b (IL-37bΔ1–45) [24]. In order to investigate the role of IL-37bΔ1–20 and IL-37bΔ1–45 in HSV-1 replication, IL-37bΔ1–20-over-expressing or IL-37bΔ1–45-over-expressing HeLa cells were infected with either HSV-1/GFP or HSV-1F. The expression of eGFP or viral protein gD-1 was notably decreased in IL-37bΔ1–45 overexpressing HeLa cells but not in IL-37bΔ1–20 overexpressing HeLa cells infected with HSV-1/GFP or HSV-1F (Fig. 2A and B). Furthermore, HSV-1 viral titers were also reduced in IL-37bΔ1–45-overexpressing cells (Fig. 2C). IL-37b primarily functions in its secreted form [25], so we next examined the anti-HSV-1 activity of rhIL-37b protein. We found that treatment with rhIL-37b significantly inhibited HSV-1 replication and the production of viral progeny (Fig. 2D and E). ACV is recognized as a first-line antiviral agent for managing clinical HSV infectious diseases, and rhIL-37b demonstrated a higher SI value-an indicator for the safe range of drug effects compared to ACV *in vitro* (Fig. 2F and G). In summary, this study identifies IL-37b as an *in vitro* anti-HSV-1 agent, suggesting that it may also be a potential candidate for the treatment of HSK.

3.3. rhIL-37b treatment blocks the development of HSK in HSV-1-infected mice

Although mice lack the homologous *Il-37* gene [10], the human IL-37 protein can activate mouse IL-18Rα and SIGIRR, which are also well-known IL-37 receptors in humans [26]. This suggests that the HSV-1-infected cornea mouse model is suitable for assessing the antiviral activity of IL-37b. Subsequently, we established a mouse model of HSV-1-infected corneas based on a previous study [2]. Initially, we confirmed that the expression levels of IL-18Rα and SIGIRR in the corneal tissue of HSK mice were consistent with those in the Mock group (Fig. 3A and B). Following this, HSV-1-infected mice received a subconjunctival injection of 1.0 μg of rhIL-37b in 10 μL in their right eyes three times to evaluate the preventive effect of rhIL-37b on the development of HSK (Fig. 3C). The body weight of HSV-1-infected mice that received the rhIL-37b subconjunctival injection was higher than that mice that received PBS (Fig. 3D). During the progression of HSK, rhIL-37b treatment significantly alleviated the extent of eyelid injury (Fig. 3E),

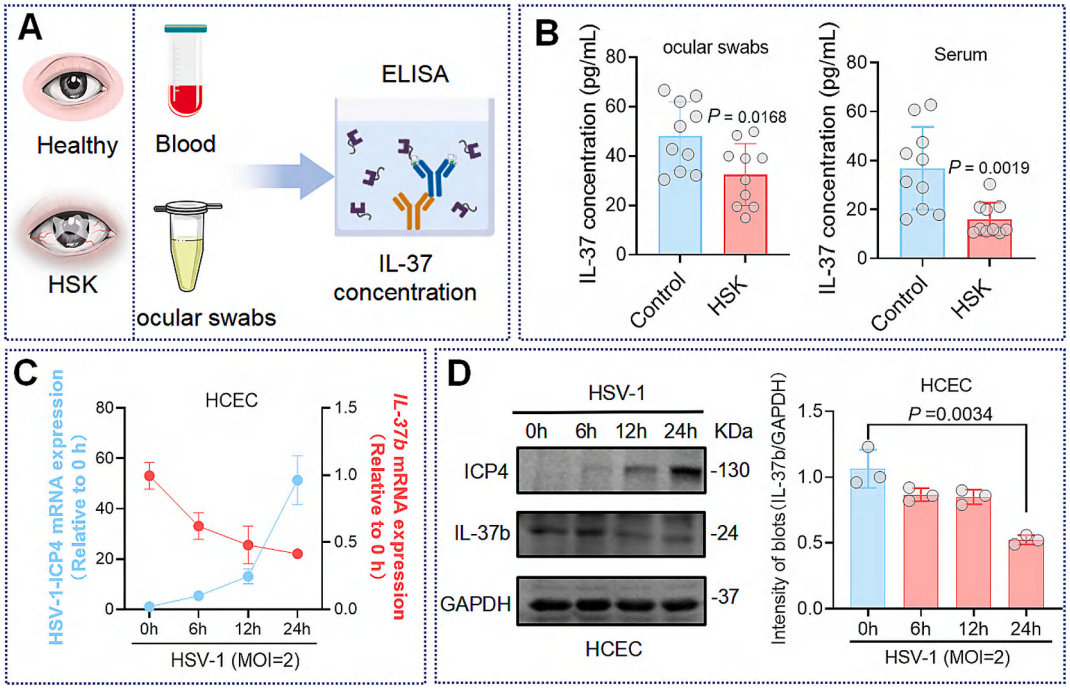

Fig. 1. IL-37 levels were decreased in HSK patients. **(A)** A graphic representation illustrates the collection of serum and ocular swabs from healthy individuals (n = 5–10) and HSK patients (n = 5–10). Serum and ocular swabs were collected for ELISA detection. **(B)** IL-37 levels in ocular swabs and serum were measured using an ELISA assay (n = 10). **(C)** *HSV-1-ICP4* and *IL-37* mRNA levels in HCEC cells infected with HSV-1 (MOI = 2) were quantified by RT-qPCR assay (n = 3). **(D)** HSV-1-ICP4 and IL-37b protein levels in HCEC cells infected with HSV-1 (MOI = 2) infection were assessed using Western blot analysis (n = 3). The intensity of the blots was analyzed using Image J software. The major statistical procedures applied were: *Shapro-Wiik* test (B—D), *F*-test (C and D), *Wilcoxon* test (B), and *Repeated Measures ANOVA* and *Kruskal-Wallis H* test (C and D).

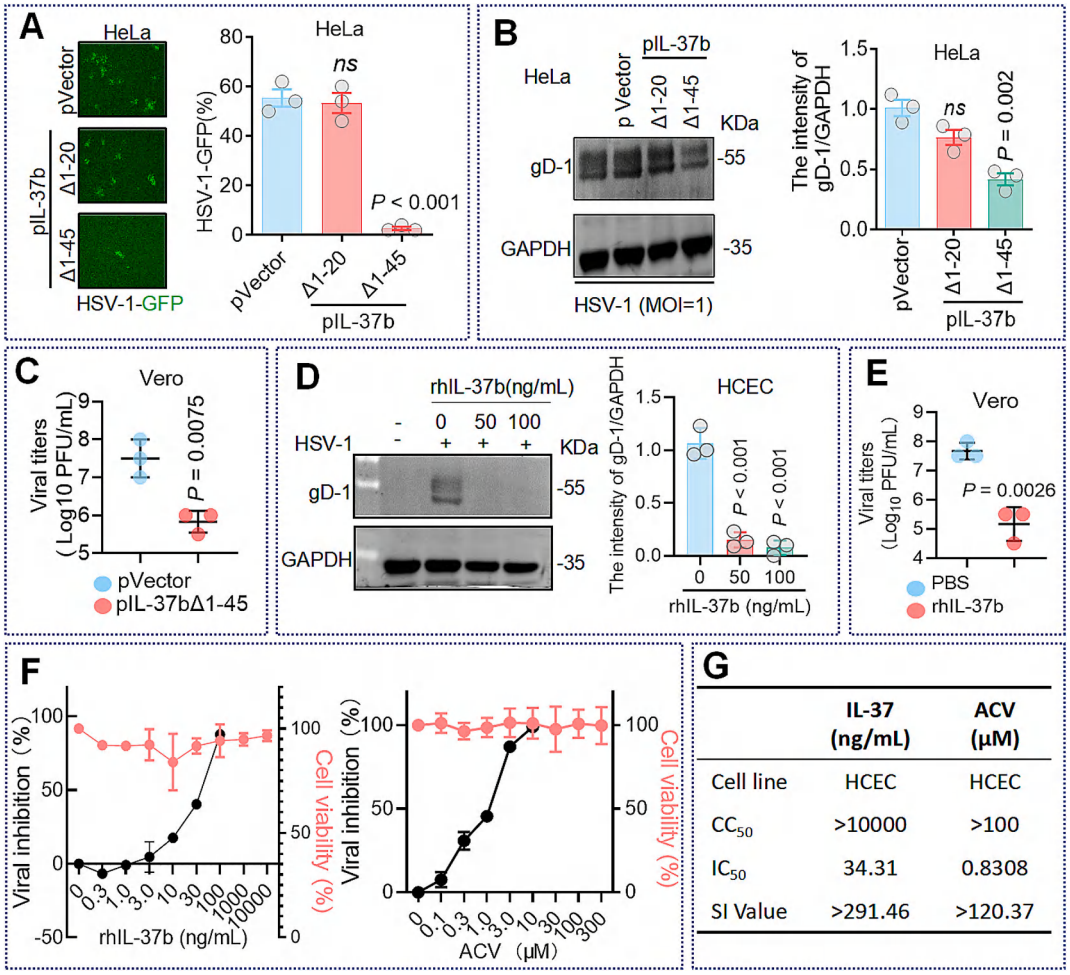

	IL-37 (ng/mL)	ACV (μM)
Cell line	HCEC	HCEC
CC_{50}	>10000	>100
IC_{50}	34.31	0.8308
SI Value	>291.46	>120.37

Fig. 2. IL-37bΔ1–45 inhibits HSV-1 replication *in vitro*. **(A-B)** HeLa cells were over-expressed with IL-37bΔ1–20 and IL-37bΔ1–45 for 24 h, respectively. They were then infected with HSV-1/GFP (MOI = 1) or HSV-1F for 24 h. Representative images were acquired by confocal microscopy ($n = 3$), and viral protein gD-1 expression was detected by Western blot assay. The relevant intensity of blots was analyzed by Image J software (n = 3). **(C)** HSV-1F viral titers were determined by plaque assay ($n = 3$). **(D)** HSV-1F-infected (MOI = 1) HCEC cells were treated with rhIL-37b (0, 50, 100 ng/mL) for 24 h, and viral protein gD-1 expression was determined by Western blot. The relevant intensity of blots was analyzed by Image J software (n = 3). **(E)** HSV-1F viral titers were determined by plaque assay (n = 3). **(F-G)** The cytotoxicity and antiviral activity of rhIL-37b and ACV were determined by the RT-qPCR assay, and CC_{50}, IC_{50}, and SI value were calculated, SI=CC_{50}/IC_{50}. The major statistical procedures applied were: *Shapro-Wiik* test (A-E), *F*-test (A, B, and D), *One-way ANOVA* and *Dunnett-t*-test (A, B, and D), *Student-t*-test (C and E), *nonlinear regression* analysis (F), *ns:* not significant.

preserved corneal morphology (Fig. 3F), and reduced both disease scores and fluorescein sodium staining scores of the eyes (Fig. 3G). HSK is an immunopathological condition that typically results from HSV-1 establishing lytic replication on the corneal surface and activating the host's inflammatory response in the cornea [4]. Additionally, rhIL-37b treatment inhibited the mRNA expression of inflammatory factors, including *Il-6*, *Il-17α*, *Ccl2*, and *Cxcl2,* in the corneal tissues of HSV-1-infected mice (Fig. 3H). Furthermore, rhIL-37b significantly reduced HSV-1 shedding from the corneal tissues of HSV-1-infected mice (Fig. 3I). These results indicate that rhIL-37b holds a promise for treating HSK by reducing corneal inflammation and inhibiting viral replication. The mechanism by which IL-37b exerts its anti-HSK effect is particularly intriguing.

3.4. rhIL-37b alleviates HSV-1-infection-induced mouse corneal injury via SIGIRR activation

IL-18Rα and SIGIRR are well-known receptors for IL-37b. We initially constructed IL-18Rα and SIGIRR knockdown HeLa cell lines using a lentiviral-delivery system to investigate whether IL-18Rα and/or SIGIRR are involved in the rhIL-37b-mediated anti-HSV-1 effects *in vitro* (Fig. 4A). The data indicate that SIGIRR knockdown, but not IL-18Rα knockdown, partially rescued viral progeny production *in vitro* (Fig. 4B and C). Next, we utilized *Sigirr*-deficient C57BL/6 J mice to further explore the therapeutic role of IL-37 in HSV-1 corneal acute infection. We established an animal model featuring acute corneal HSV-1 infection in both *Sigirr*-deficient mice and wide type (*Wt*) mice to observe the effects of the virus under different genetic conditions (Fig. 4D). The data showed that HSV-1-infected *Sigirr*-deficient mice did not exhibit statistically significant differences in body weight (Fig. 4E), corneal morphology (Fig. 4F), disease scores (Fig. 4G **left**), fluorescein sodium scores (Fig. 4G **right**), and viral titers in ocular swabs (Fig. 4H) compared to *Wt* mice infected with HSV-1. This indicates that *Sigirr* gene deficiency did not affect the progression of HSK in mouse HSV-1 corneal infection model. We further administered rhIL-37b *via* subconjunctival injection to assess its therapeutic effect of rhIL-37b on *Sigirr*-deficient mice with HSV-1 corneal infection (Fig. 4I). Following rhIL-37b treatment, we observed greater body weight loss (Fig. 4J) and more severe corneal injury (Fig. 4K), along with higher associated scores (Fig. 4L) in *Sigirr*-deficient mice compared to *Wt* mice. Furthermore, the anti-HSV-1 effect of rhIL-37b was abolished in *Sigirr*-deficient mice (Fig. 4M). In conclusion, both *in vitro* and *in vivo* studies have demonstrated the

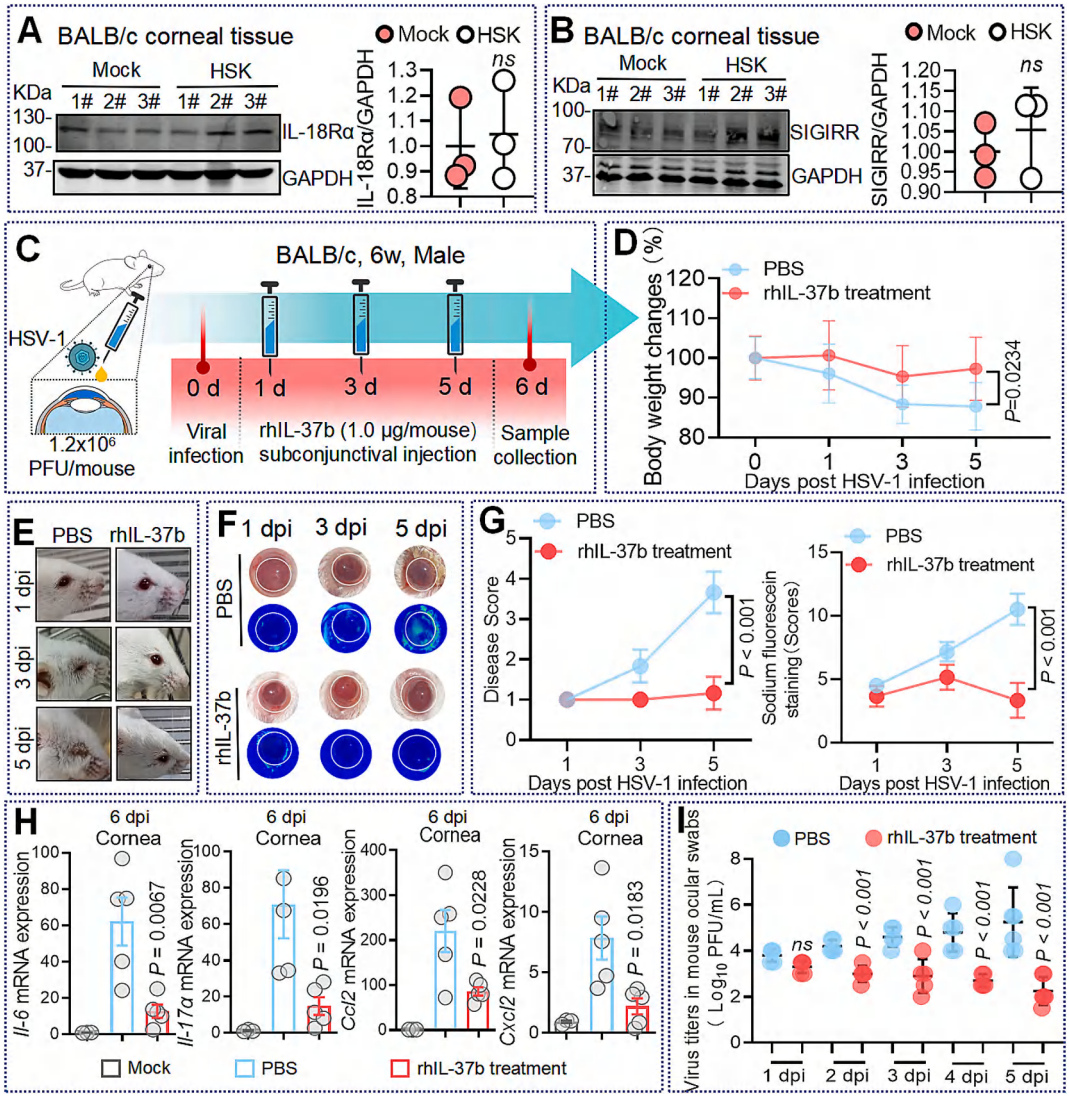

Fig. 3. rhIL-37b alleviates HSV-1 induced corneal injury. **(A-B)** Western blot assay was used to detected IL-18Rα and SIGIRR expression in HSK and Mock mice. The relative intensities of the blots were analyzed using Image J software (n = 3). **(C)** Schematic diagram of the protocol for establishing the HSV-1-infected mouse model treated with PBS and rhIL-37b, respectively. rhIL-37b (1.0 μg/mouse) was administered by subconjunctival injection at 1 dpi, 3 dpi, and 5 dpi. **(D)** Body weight changes of the HSK mice were recorded from the PBS and rhIL-37b treatment groups, respectively ($n = 5$). **(E)** Representative photographs of the right eyes of HSV-1-infected mice with PBS or rhIL-37b treatment at 1 dpi, 3 dpi, and 5 dpi ($n = 3$). **(F)** Corneal tissues were stained with fluorescein sodium or left unstained at 1 dpi, 3 dpi, and 5 dpi, and representative corneal morphology images were obtained using a stereomicroscope. **(G)** The ocular disease scores and fluorescein sodium staining scores were analyzed under the stereomicroscope ($n = 5$). **(H)** mRNA expression of *Il-6, Il-17α, Ccl-2,* and *Cxcl-2* in HSV-1-infected corneal tissues at 6 dpi from PBS and rhIL-37 treatments was determined by RT-qPCR assay (n = 5). **(I)** HSV-1F viral titers in ocular swabs of mice were determined by plaque assay (n = 5). The major statistical procedures applied were: *Shapro-Wiik* test (A, B, D, G, H, and I), *F*-test (D, G, H, and I), *Wilcoxon* test (A and B), *Repeated measures ANOVA* and *Dunnett-t*-test (D, G, and I), *Kruskal-Wallis H* test and *Dunnett-t*-test (H). *ns:* not significant.

crucial role of the IL-37/SIGIRR pathway in the treatment of HSV-1 corneal infection.

Although treatment with rhIL-37b has shown promise in controlling the development of HSK, continuous administration is still required. Additionally, frequent topical ocular drug injections can result in poor patient compliance [27]. Therefore, it is essential to develop a therapeutic strategy that provides a long-acting profile, capitalizing on the anti-HSK potential of IL-37b.

3.5. *AAV9-IL-37bΔ1–45 gene therapy alleviates HSV-1 infection-induced mouse corneal injury*

AAV9 delivery system is a widely utilized viral vector platform recognized for its ability to effectively transduce various tissues, including the corneal tissue, making it an attractive tool for gene therapy applications [28]. Since mice are known to lack a homologous gene for IL-37, we aim to transfect the human *Il-37bΔ1–45* gene into the mouse corneal tissue to further evaluate the therapeutic role of IL-37b in the development of HSK (Fig. 5A). Firstly, we confirmed that the *Il-37bΔ1–45* gene was successfully expressed in corneal tissues (flag-tag, red) after three weeks AAV9-IL-37bΔ1–45 infection (Fig. 5B). Furthermore, the signal of AAV9 labeled with eGFP (green) was detected in both the cornea and retina (Fig. 5C). Next, we assessed the potential adverse effects of the AAV9-IL-37bΔ1–45 system in mice prior to HSV-1 corneal infection. We observed that the administration of AAV9-IL-37bΔ1–45 did not affect the corneal morphology or the body weight of the mice (Fig. 5D). Splenic morphology and splenic index can indirectly reflect the systemic inflammatory response; however, the splenic morphology and splenic index remained unchanged following AAV9-IL-37bΔ1–45 administration (Fig. 5E). Furthermore, the ratio of red to white pulp also

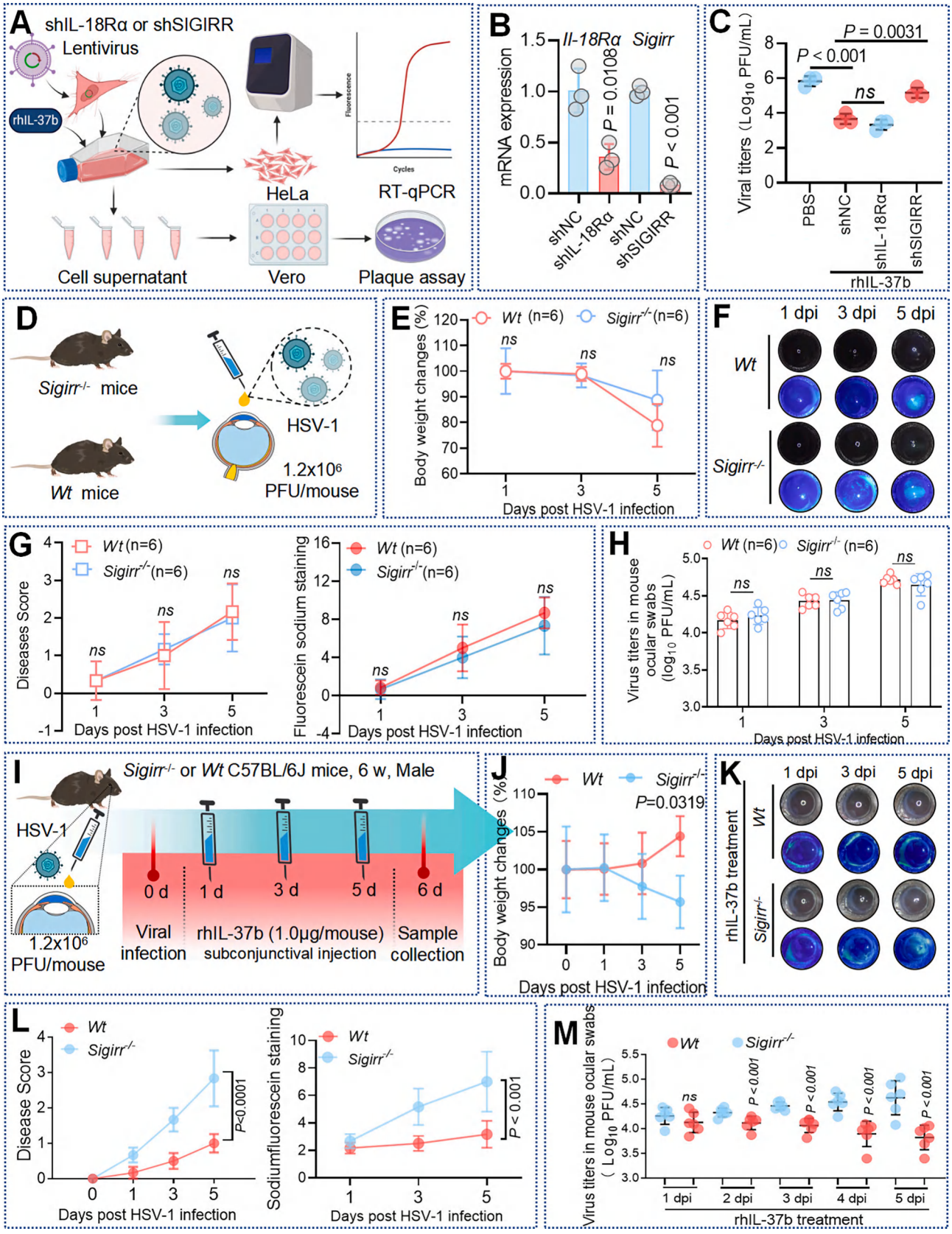

(caption on next page)

Fig. 4. rhIL-37b alleviates HSV-related corneal injury *via* SIGIRR pathway. **(A)** Schematic diagram illustrating the experimental setup. Lentiviruses were utilized to transfect shIL-18Rα, shSIGIRR, and shNC into HeLa cells, followed by infection with HSV-1F in the presence or absence of rhIL-37b treatment (50 ng/mL) ($n = 3$). **(B)** RT-qPCR assay was used to detect *Il-18Rα and Sigirr* mRNA expression. **(C)** HSV-1F viral loads were quantified *via* plaque assay (n = 3). **(D)** Schematic representation outlining the modeling protocol for HSV-1 infection in *Sigirr*$^{-/-}$ mice and *Wt* mice. **(E)** Changes in body weight between *Sigirr*$^{-/-}$ mice and *Wt* mice post-HSV-1 infection were monitored at 1 dpi, 3 dpi, and 5 dpi ($n = 6$). **(F)** Corneal tissues underwent fluorescein sodium staining, and representative images capturing corneal morphology were obtained using a stereomicroscope at 1 dpi, 3 dpi, and 5 dpi (n = 3). **(G)** Disease severity scores and fluorescein sodium staining intensities were evaluated (n = 6). **(H)** Viral titers of HSV-1F in mouse ocular swabs were measured through plaque assay (n = 6). **(I)** Schematic diagram detailing the protocol for establishing HSV-1 infection in *Sigirr*$^{-/-}$ mice and subsequent treatment with rhIL-37b. 6-week-old male *Wt* or *Sigirr*$^{-/-}$ mice were inoculated with HSV-1F (1.2×10^6 PFU/mouse), followed by subconjunctival injections of rhIL-37b (1.0 μg/mouse) at 1 dpi, 3 dpi, and 5 dpi. **(J)** Body weight fluctuations were documented at 0 dpi, 1 dpi, 3 dpi, and 5 dpi (n = 5). **(K)** Corneal tissues were stained with fluorescein sodium or unstained at 1 dpi, 3 dpi, and 5 dpi (n = 3). Representative images of corneal morphology were captured under the stereomicroscope. **(L)** Disease scoring and fluorescein sodium staining assessments were additionally carried out (n = 5). **(M)** HSV-1F viral titers within mouse ocular swabs were once more determined by plaque assay (n = 5). The major statistical procedures applied were: *Shapro-Wiik* test (B, C, E, G, H, J, L, and M), *F*-test (C, E, G, H, J, L, and M), *Repeated measures ANOVA* and *Dunnett-t*-test (E, G, H, J, L, and M), *paired-t*-test (B), *one-way ANOVA* and *SNK-q* test (C). *ns:* not significant.

indicates the systemic immune response, which is also remained unchanged in the spleen tissues of mice that were administered AAV9-IL-37bΔ1–45 (Fig. 5F). The evidence presented suggests that AAV9-IL-37bΔ1–45 has an acceptable safety profile at a target mouse dose of 1.0×10^{11} v.g.

We further evaluated the therapeutic role of AAV9-IL-37bΔ1–45 in mouse corneal injury associated with HSV-1 infection. Following HSV-1 corneal infection, the administration of AAV9-IL-37bΔ1–45 not only protected the mice from body weight loss (Fig. 5G) but also alleviated corneal injury (Fig. 5H and I). Additionally, AAV9-IL-37bΔ1–45 significantly inhibited the production of viral progeny in the ocular swabs of mice infected with HSV-1 (Fig. 5K). Overall, AAV9-IL-37bΔ1–45 transduction represents a promising strategy for targeted preventive delivery in HSK, with the potential to enhance antiviral effects during the acute exacerbation of disease induced by HSV-1 infection.

3.6. Administration of AAV9-IL-37bΔ1–45 and rhIL-37b both alleviate corneal injury in recurrent HSK mice

The prevention and treatment of recurrent HSK pose a significant clinical challenge [3]. We established a recurrent HSK mouse model according to a previous study [29] to investigate, in parallel, the preventive role of AAV9-delivered *Il-37bΔ1–45* gene and the therapeutic role of rhIL-37b in this model (Fig. 6A). AAV9 is widely prevalent in humans, suggesting that human pooled serum may contain substantial levels of neutralizing antibodies against AAV9 vector. First, we compared the mRNA expression of *Il-37b* in the corneas of AAV9-IL-37b-treated HSK mice and AAV9-IL-37b-treated recurrent HSK mice to investigate the impact of human pooled serum on the transfection efficiency of the AAV9 vector *in vivo*. Mice in both the HSK model and the recurrent HSK model were administered AAV9-IL-37b (1.0×10^{11} v.g.) for 3 weeks and subsequently infected with HSV-1 for 6 days. Importantly, recurrent HSK mice received 1 mL of human pooled serum *via* intraperitoneal injection prior to the AAV9 vector injection. Compared to the AAV9-IL-37b-treated HSK mice, the expression of *Il-37b* mRNA was lower in the corneal tissues of AAV9-IL-37b-treated recurrent HSK mice (Fig. 6B). Next, we conducted an *in vitro* experiment to confirm the impact of human pooled serum on the transfection efficiency of the AAV9 vector. AAV9-IL-37b (MOI = 10) was co-incubated with PBS (1×) or human serum (500 μL) at 37 °C for 1 h, and subsequently used to infect MEFs for 36 h. The results indicated that the co-incubation of AAV9-IL-37b with human pooled serum resulted in lower *Il-37b* mRNA expression in MEFs compared to co-incubation with PBS (1×) (Fig. 6C). Compared to the recurrent HSK group, a higher body weight was observed in both the AAV9-IL-37bΔ1–45 preventive administration group and rhIL-37b treatment group (Fig. 6D). Furthermore, both AAV9-IL-37bΔ1–45 and rhIL-37b administration alleviated corneal injury and reduced the disease score of the eyes and decreased fluorescein sodium staining scores in recurrent HSK mice (Fig. 6E and F). AAV9-IL-37bΔ1–45 and rhIL-37b administration also mitigated corneal thickening observed in recurrent HSK mice (Fig. 6G), which may be associated with lower levels of HSV-1 particle production in ocular swabs from the recurrent HSK mice (Fig. 6H). Our data illustrate that AAV9-delivery of the *Il-37bΔ1–45* gene could serve as a potential strategy for preventing recurrent HSK following antiviral treatment of an acute episode. Additionally, rhIL-37b was identified as a potential therapeutic molecule for treating recurrent HSK in this study.

4. Discussion

HSV-1 is one of the most prevalent viruses in humans, with an estimated 50–80 % of the global population infected [30]. Infection of the cornea by HSV-1 can lead to HSK, with recurrent episodes potentially leading to blindness [31]. Acyclovir and ganciclovir are the first-line medications for the treatment of HSK; however, they often fail to prevent recurrent episodes due to factors such as viral latency, inadequate dosing, or poor patient compliance [32]. Furthermore, the increased frequency and severity of HSV reactivation necessitate timely administration of these drugs, which can compromise their effectiveness. There is an urgent need to develop strategies aimed at preventing recurrent HSK by intervening before the reactivation of HSV following acute episodes. Currently, treatment with rhIL-37b protein has been shown to alleviate corneal injury in mice experiencing both HSK acute and recurrent episodes of HSK through the IL-37/SIGIRR signaling pathway. Notably, AAV9-mediated delivery of the *Il-37b* gene has been identified as an effective strategy for preventing recurrent HSK in this study.

Mice lack the Il-37 homologous gene, which hinders our ability to investigate the relationship between HSV-1 corneal infection and IL-37 expression in mouse models. However, mouse IL-18Rα and/or SIGIRR can transduce the anti-inflammatory signals of human IL-37 [33]. The roles of human IL-37 protein have been extensively studied using mouse models across various disease contexts, providing an opportunity to investigate the biological functions of IL-37 *in vivo*. Currently, the *in vivo* experiments examining the role of IL-37b in recurrent HSK have only been conducted in BALB/c and C57BL/6 J mouse models. It is challenging to determine whether the anti-HSK effects mediated by rhIL-37 observed in this study would be replicated in an animal model that possesses its own *Il-37* homologous gene. Several well-established animal models exist for studying HSK, including mice, guinea pigs, and rabbits. To date, it remains uncertain whether guinea pigs possess an *Il-37* homologous gene, while the IL-37 protein has been detected in rabbit serum [34]. Although no studies have investigated the role of rabbit IL-37 in HSK models, rhIL-37 has been shown to mediate an anti-inflammatory response in rabbit models [35], which aligns with findings in mouse models. It is essential to develop additional HSK models in various animal species to further confirm the anti-HSK effects of IL-37b. In summary, the therapeutic roles of IL-37b in the HSK mouse model studied in this study should be interpreted with caution.

In this study, we demonstrated that the anti-HSV-1 effect of IL-37b resulted from either rhIL-37b protein treatment or AAV9-IL-37bΔ1–45 transfection, both of which significantly reduced viral load *in vitro* and *in vivo* [36]. The mechanisms underlying the preventive and therapeutic

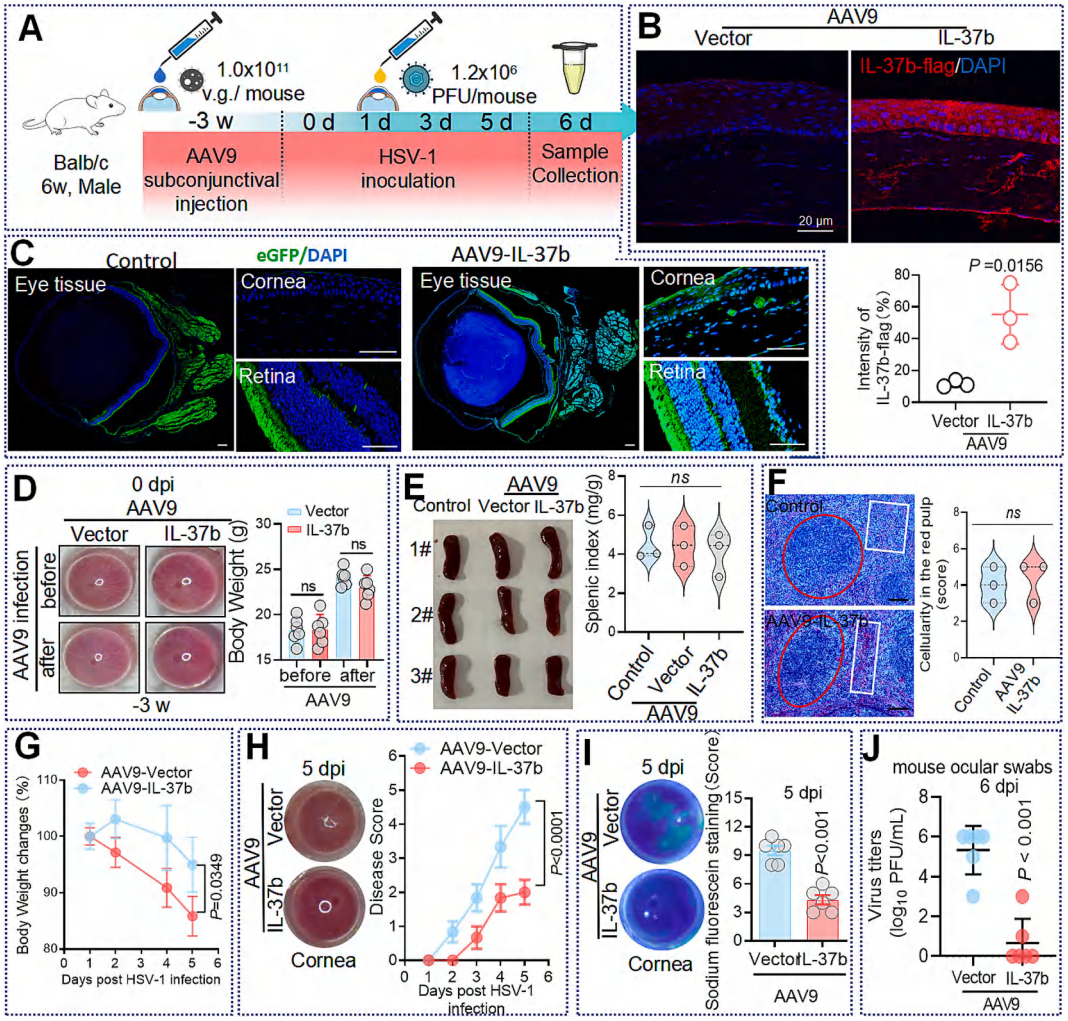

Fig. 5. AAV9-IL-37bΔ1–45 alleviates HSV-1 induced corneal injury. **(A)** Schematic diagram illustrating the protocol for AAV9-IL-37bΔ1–45 pre-treatment (1.0×10^{11} v.g.) in mice followed by HSV-1 (1.2×10^{6} PFU/mouse) infection. **(B)** Representative immunofluorescence (IF) images depicting IL-37b expression (flag-tag in red) in corneal tissues following AAV9-IL-37bΔ1–45 administration after 3 weeks ($n = 3$). **(C)** IF assay was employed to ascertain AAV9 (eGFP, green) expression localization in both corneal and retinal tissues of mice, with and without AAV9-IL-37bΔ1–45 treatment, at 6 dpi. **(D)** Representative images of corneal morphology from AAV9-vector infected and AAV9-IL-37bΔ1–45 infected mice were captured under a stereomicroscope at 0 dpi (n = 3). Concurrently, body weights of these mice were documented ($n = 6$). **(E)** Photographs of spleens from AAV9-vector and AAV9-IL-37bΔ1–45 infected mice, uninfected with HSV-1, are shown; the splenic index was calculated as the ratio of spleen weight to body weight (mg/g). **(F)** Representative hematoxylin and eosin (H&E) stained sections of spleen tissues from AAV9-vector and AAV9-IL-37bΔ1–45 infected mice, devoid of HSV-1 infection, are presented. Quantification methodologies are detailed in the methods section, with red circles indicating red pulp and white boxes demarcating white pulp. **(G)** Body weight changes of the HSV-1-infected mice treated with AAV9-Vector or AAV9-IL-37bΔ1–45 were recorded (n = 6). **(H)** Corneal morphology images from HSV-1 infected mice undergoing treatment with AAV9-vector or AAV9-IL-37bΔ1–45 were acquired under the stereomicroscope at 5 dpi (n = 3), while disease scoring was conducted at 1, 2, 3, 4, and 5 dpi (n = 6). **(I)** Fluorescein sodium-stained corneal tissue images from HSV-1 infected mice treated with AAV9-vector or AAV9-IL-37bΔ1–45 were gathered under the stereomicroscope and assessed for fluorescein sodium staining intensity (n = 6). **(J)** Viral loads of HSV-1F in mouse ocular swabs were quantified through plaque assays (n = 6). The major statistical procedures applied were: *Shapro-Wiik* test (B, D—I, and J), *F*-test (E, G and H), *Wilcoxon* test (B), *paired-t*-test (D), *one-way ANOVA* and *SNK-q* test (E), *Repeated measures ANOVA* and *Dunnett-t*-test (G and H), *Student-t*-test (F, I, and J). *ns:* not significant. (For interpretation of the references to colour in this figure legend, the reader is referred to the web version of this article.)

effects of IL-37b for the recurrent HSK are particularly intriguing. Aside from IL-18Rα and/or SIGIRR, no other membrane receptors for the IL-37 protein have been identified. IL-37 initially binds to the cell membrane receptor IL-18Rα and recruits SIGIRR to form a ternary complex, which subsequently activates a series of intracellular signaling cascades [33]. Given thecritical roles of IL-18Rα and SIGIRR in IL-37 signaling transduction, we further confirmed that the activation of SIGIRR, rather than IL-18Rα, is essential for in IL-37b-induced HSV inhibition. The IL-37/SIGIRR pathway is a well known anti-inflammation mechanism [10]. For instance, the activation of the IL-37/SIGIRR pathway is associated with the inhibition of Smad3-induced STATs, which further suppresses the NF-κB pathway [37]. NF-κB activation is crucial for HSV-1 replication [38,39], and NF-κB is considered as a antiviral target for the treatment of HSV-1-related diseases [40]. Moreover, HSV-1-associated inflammation is also dependent on NF-κB activation [41]. Based on the evidence presented, we speculate that the anti-HSV-1 effects of IL-37/SIGIRR may be associated with the inhibition of NF-κB pathway.

HSK-induced vision impairment primarily results from recurrent HSK episodes that lead to corneal scarring [42]. Recurrent HSK presents an urgent clinical challenge that necessitates effective intervention. Conventional treatments, such as acyclovir and ganciclovir, offer only short-lived efficacy through eye drops that require frequent administration, resulting in limited control over recurrent HSK [43]. Consequently, preventative strategies are essential for individuals with a

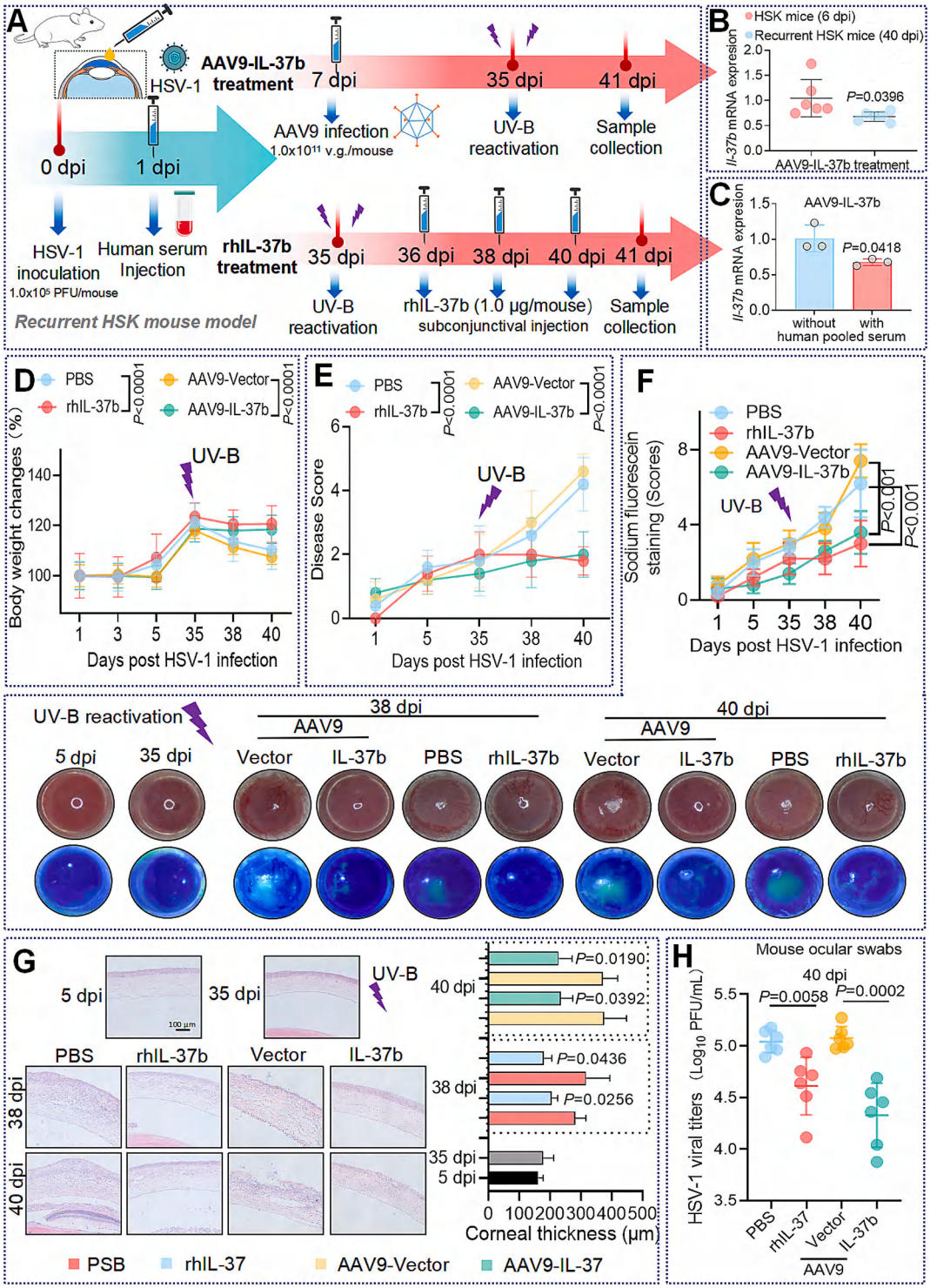

Fig. 6. AAV9-IL-37bΔ1–45 gene therapy and rhIL-37b treatment both alleviate corneal injury in recurrent HSK mice. **(A)** A flow diagram illustrates the experimental setup where recurrent HSK mice were divided into two distinct groups. And mice in these groups were then treated with AAV9-IL-37bΔ1–45 or rhIL-37b, respectively. **(B)** The mRNA expression of *Il-37b* was analyzed in the corneal tissues of AAV9-IL-37b-treated HSK mice at 6 dpi and in AAV9-IL-37b-treated recurrent HSK mice at 40 dpi. The recurrent HSK mice received a pretreatment of 1 mL of human serum one week prior to the AAV9-IL-37b treatment. **(C)** AAV9-IL-37b (MOI = 10) was co-incubated with PBS (1×) or human serum (500 μL) at 37 °C for 1 h, and then used to infect MEFs for 36 h. he mRNA expression of *Il-37b* was analyzed by RT-qPCR assay. **(D)** The body weight changes of the mice were recorded at 1 dpi, 3 dpi, 5 dpi, 35 dpi, 38 dpi, and 40 dpi (n = 6). **(E)** The disease scores of mice administered AAV9-IL-37bΔ1–45, AAV9-Vector, PBS, or rhIL-37b were evaluated at 1 dpi, 5 dpi, 35 dpi, 38 dpi, and 40 dpi. **(F)** Corneal tissues were either stained with fluorescein sodium or left unstained in mice treated with AAV9-IL-37bΔ1–45, AAV9-Vector, PBS, or rhIL-37b at 5, 35, 38, and 40 dpi (n = 3). Representative images of corneal morphology were captured using a stereomicroscope. Additionally, fluorescein sodium staining scores were analyzed (n = 6). **(G)** Representative H&E images of corneal tissues obtained from the recurrent HSK mice with rhIL-37b treatment or AAV9-IL-37bΔ1–45 treatment at 5 dpi, 35 dpi, 38 dpi, and 40 dpi. Corneal thickness quantification was analyzed by Image J software (n = 3) **(H)** The viral titers of HSV-1F in mouse ocular swabs were determined using a plaque assay (n = 6). The major statistical procedures applied were: *Shapro-Wiik* test (B—H), *F*-test (D—F, and H), *Wilcoxon* test (B and C), *Repeated measures ANOVA* and *SNK-q* test (D—F), *paired-t-test* (G), *one-way ANOVA* and *SNK-q* test (H) *ns:* not significant.

history of recurrent HSK [44]. The AAV9 delivery system is a powerful gene therapy tool that effectively transduces targeted therapeutic genes into specific cells. The system offers advantages in terms of stability and longevity, which are particularly beneficial for treating diseases, including recurrent HSK, where sustained gene expression is crucial. We employed AAV9 to establish stable, long-term expression of IL-37b in the ocular tissues of mice, aiming to prevent the recurrent HSK. Currently, AAV9-IL-37b gene therapy demonstrates a strong preventative effect on recurrent HSK by alleviating corneal injury and inhibiting HSV reactivation. These findings suggest that sustained IL-37b expression contributes to preventing HSK development.

In the recurrent HSK mouse model, human pooled serum is employed to suppress initial HSK infection and facilitate the establishment of HSV-1 latency within the trigeminal ganglia. However, AAV9 is quite prevalent in humans, suggesting that pooled serum may contain significant levels of neutralizing antibodies against the AAV9 vector. Our results showed that human pooled serum co-incubated with AAV9-IL-37b decreased *Il-37b* mRNA expression by approximately 30 % in MEFs. The findings suggests that alternative strategies or modifications to the AAV9 vector may be necessary to ensure its high transfection efficiency in the treatment of human HSK in the future.

Approximately 40 % of HSK patients experience 2 to 5 relapses over their lifetime, while 11 % experience 6 to 15 relapses [45]. Therefore, the long-term efficacy of gene therapy utilizing the AAV9 delivery system in corneal tissue warrants consideration. Although we have not conducted extend longer-term follow-up observations on the expression of IL-37 in mouse corneal tissues delivered by AAV9, existing research indirectly indicates that the AAV9 vector can sustain target gene expression in mouse corneal tissue for at least 200 days [15]. Hao F et al., demonstrated that intrastriatal injection of AAV9 vectors resulted in a robust and widespread expression of the target gene in the injected striatum of rats for up to 24 weeks [46]. Furthermore, AAV9-mediated gene replacement therapy has been administered in the treatment of spinal muscular atrophy (SMA), with the therapeutic effects maintained for 4.6 to 5.6 years following AAV9 vector infusion in SMA patients [47]. This suggests a promising potential for the clinical translation of the AAV9 delivery system in preventing the development of recurrent HSK. Although our current study does not provide direct observational data for longer durations, previous findings and supporting literature lead us to believe that AAV9 therapy may offer long-lasting and sustained efficacy in preventing recurrent HSK.

In summary, our data provide evidence that IL-37bΔ1–45 functions as an anti-HSV factor. AAV9-IL-37bΔ1–45 gene therapy shows promise as a potential preventive therapeutic option for the recurrent HSK. By shifting the focus from symptomatic treatment to a more durable preventative strategy, we aim to establish new standards in the management of recurrent HSK.

Funding

This work was supported by the National Natural Science Foundation of China (81900823) and the Research Foundation for Advanced Talents (bsqd2024011 to D.C.) from Bengbu Medical University.

CRediT authorship contribution statement

Jing Wu: Writing – original draft, Validation, Software, Project administration, Methodology, Investigation, Data curation. **Ye Liu:** Writing – review & editing, Methodology, Investigation, Data curation. **Chenchen Wang:** Visualization, Software, Project administration, Conceptualization. **Yurong Cai:** Software, Data curation. **Xiaomin Zhu:** Resources, Formal analysis. **Ruining Lyu:** Software, Investigation, Data curation. **Qiao You:** Validation, Project administration. **Xiaoqian Liu:** Project administration, Formal analysis. **Qin Qin:** Writing – review & editing, Visualization, Resources, Investigation, Data curation. **Yajie Qian:** Writing – review & editing, Software, Resources, Investigation, Conceptualization. **Deyan Chen:** Writing – review & editing, Writing – original draft, Project administration, Methodology, Investigation, Funding acquisition, Data curation, Conceptualization.

Declaration of competing interest

Authors declare that they have no competing interests.

Acknowledgments

We would like to express our gratitude to Prof. Damo Xu (Shenzhen University, Shenzhen, China), for providing the *SIGIRR*-deficient mice used in our current study [20]. We also extend our thanks to Prof. Lining Zhang (School of Basic Medicine Sciences, Shandong University, Jinan, China) for generously supplying the plasmids expressing IL-37bΔ1-45 and IL-37bΔ1-20 [48]. Additionally, we appreciate Prof. Zhiwei Wu and Prof. Zhiqiang Huang (Nanjing University, Nanjing, China) for their valuable suggestions on the manuscript. Finally, we thank the Public Technology Service Center at Fujian Medical University for giving their technical support in this study.

Appendix A. Supplementary data

Supplementary data to this article can be found online at https://doi.org/10.1016/j.jconrel.2025.113600.

Data availability

Data will be made available on request.

References

[1] M.E. Marcocci, et al., Herpes simplex Virus-1 in the brain: the dark side of a sneaky infection, Trends Microbiol. 28 (10) (2020) 808–820.
[2] H. Xu, et al., Harmol used for the treatment of herpes simplex virus induced keratitis, Virol. J. 21 (1) (2024) 118.
[3] F. Antony, et al., The immunobiology of corneal HSV-1 infection and herpetic stromal keratitis, Clin. Microbiol. Rev. 37 (3) (2024) e0000624.
[4] J. Ren, et al., Role of innate interferon responses at the ocular surface in herpes simplex virus-1-induced herpetic stromal keratitis, Pathogens 12 (3) (2023).
[5] S.J. Park, et al., Herpesvirus entry mediator binding partners mediate immunopathogenesis of ocular herpes simplex virus 1 infection, mBio 11 (3) (2020).
[6] J.L. Coleman, D. Shukla, Recent advances in vaccine development for herpes simplex virus types I and II, Hum. Vaccin. Immunother. 9 (4) (2013) 729–735.
[7] M.E. Marcocci, et al., The amphibian antimicrobial peptide Temporin B inhibits in vitro herpes simplex virus 1 infection, Antimicrob. Agents Chemother. 62 (5) (2018).
[8] D. Chen, et al., 6-Thioguanine inhibits herpes simplex virus 1 infection of eyes, Microbiol. Spectr. 9 (3) (2021) e0064621.
[9] S. Kumar, et al., Identification and initial characterization of four novel members of the interleukin-1 family, J. Biol. Chem. 275 (14) (2000) 10308–10314.
[10] H. Jia, J. Liu, B. Han, Reviews of Interleukin-37: functions, receptors, and roles in diseases, Biomed. Res. Int. 2018 (2018) 3058640.
[11] C.A. Nold-Petry, et al., IL-37 requires the receptors IL-18Rα and IL-1R8 (SIGIRR) to carry out its multifaceted anti-inflammatory program upon innate signal transduction, Nat. Immunol. 16 (4) (2015) 354–365.
[12] S. Samarani, et al., The anti-inflammatory IL-37/SIGIRR axis is functionally compromised in HIV infection, Aids 33 (11) (2019) 1693–1703.
[13] M. Wels, et al., Challenges and strategies for the delivery of biologics to the cornea, J. Control. Release 333 (2021) 560–578.
[14] J.C. Grieger, S.M. Soltys, R.J. Samulski, Production of recombinant adeno-associated virus vectors using suspension HEK293 cells and continuous harvest of vector from the culture media for GMP FIX and FLT1 clinical vector, Mol. Ther. 24 (2) (2016) 287–297.
[15] J. O'Callaghan, et al., Matrix metalloproteinase-3 (MMP-3)-mediated gene therapy for glaucoma, Sci. Adv. 9 (16) (2023) eadf6537.
[16] G. Allam, et al., The potential role of interleukin-37 in infectious diseases, Int. Rev. Immunol. 39 (1) (2020) 3–10.
[17] S.A. McClellan, et al., Thrombomodulin protects against bacterial keratitis, is anti-inflammatory, but not Angiogenic, Invest. Ophthalmol. Vis. Sci. 56 (13) (2015) 8091–8100.
[18] X. Huang, et al., SIGIRR promotes resistance against *Pseudomonas aeruginosa* keratitis by down-regulating type-1 immunity and IL-1R1 and TLR4 signaling, J. Immunol. 177 (1) (2006) 548–556.

[19] Z. Wang, et al., Interleukin-37 promotes colitis-associated carcinogenesis via SIGIRR-mediated cytotoxic T cells dysfunction, Signal Transduct. Target. Ther. 7 (1) (2022) 19.
[20] R. Wei, et al., The nuclear cytokine IL-37a controls lethal cytokine storms primarily via IL-1R8-independent transcriptional upregulation of PPARγ, Cell. Mol. Immunol. 20 (12) (2023) 1428–1444.
[21] Z. Luo, et al., Inhibitory effects of baicalein against herpes simplex virus type 1, Acta Pharm. Sin. B 10 (12) (2020) 2323–2338.
[22] P. Marsh, S.C. Pflugfelder, Topical nonpreserved methylprednisolone therapy for keratoconjunctivitis sicca in Sjögren syndrome, Ophthalmology 106 (4) (1999) 811–816.
[23] J. Wu, et al., Pralatrexate inhibited the replication of varicella zoster virus and vesicular stomatitis virus: an old dog with new tricks, Antivir. Res. 221 (2024) 105787.
[24] X. Wang, et al., IL-37bDelta1-45 suppresses the migration and invasion of endometrial cancer cells by targeting the Rac1/NF-kappaB/MMP2 signal pathway, Lab. Investig. 101 (6) (2021) 760–774.
[25] A.M. Bulau, et al., Role of caspase-1 in nuclear translocation of IL-37, release of the cytokine, and IL-37 inhibition of innate immune responses, Proc. Natl. Acad. Sci. USA 111 (7) (2014) 2650–2655.
[26] A. Sánchez-Fernández, et al., IL-37 exerts therapeutic effects in experimental autoimmune encephalomyelitis through the receptor complex IL-1R5/IL-1R8, Theranostics 11 (1) (2021) 1–13.
[27] W. Chang, et al., Multifunctional Nanotherapeutics with long-acting release against macular degeneration by minimally invasive administration, ACS Nano 18 (30) (2024) 19649–19662.
[28] N. Gao, et al., CXCL10 suppression of hem- and lymph-angiogenesis in inflamed corneas through MMP13, Angiogenesis 20 (4) (2017) 505–518.
[29] M. Aubert, et al., Gene editing for latent herpes simplex virus infection reduces viral load and shedding in vivo, Nat. Commun. 15 (1) (2024) 4018.
[30] T.J. Liesegang, Herpes simplex virus epidemiology and ocular importance, Cornea 20 (1) (2001) 1–13.
[31] D. Yin, et al., Targeting herpes simplex virus with CRISPR-Cas9 cures herpetic stromal keratitis in mice, Nat. Biotechnol. 39 (5) (2021) 567–577.
[32] I. Zhang, Z. Hsiao, F. Liu, Development of genome editing approaches against herpes simplex virus infections, Viruses 13 (2) (2021).
[33] Y. Chen, et al., IL-37 attenuates platelet activation and thrombosis through IL-1R8 pathway, Circ. Res. 132 (9) (2023) e134–e150.
[34] C. Shaoyuan, et al., Increased IL-37 in atherosclerotic disease could be suppressed by atorvastatin therapy, Scand. J. Immunol. 82 (4) (2015) 328–336.
[35] P. Yan, et al., Interleukin-37 (IL-37) suppresses pertussis toxin-induced inflammatory myopathy in a rat model, Med. Sci. Monit. 24 (2018) 9187–9195.
[36] C.H. Heldin, A. Moustakas, Role of Smads in TGFβ signaling, Cell Tissue Res. 347 (1) (2012) 21–36.
[37] Y. Xie, et al., Interleukin-37 suppresses ICAM-1 expression in parallel with NF-κB down-regulation following TLR2 activation of human coronary artery endothelial cells, Int. Immunopharmacol. 38 (2016) 26–30.
[38] F. Marino-Merlo, et al., HSV-1-induced activation of NF-κB protects U937 monocytic cells against both virus replication and apoptosis, Cell Death Dis. 7 (9) (2016) e2354.
[39] P. Tajpara, et al., A preclinical model for studying herpes simplex virus infection, J. Invest. Dermatol. 139 (3) (2019) 673–682.
[40] X. Chen, et al., *Houttuynia cordata* blocks HSV infection through inhibition of NF-κB activation, Antivir. Res. 92 (2) (2011) 341–345.
[41] S. Takeda, et al., Roles played by toll-like receptor-9 in corneal endothelial cells after herpes simplex virus type 1 infection, Invest. Ophthalmol. Vis. Sci. 52 (9) (2011) 6729–6736.
[42] L. Wang, et al., Pathogenesis of herpes stromal keratitis: immune inflammatory response mediated by inflammatory regulators, Front. Immunol. 11 (2020) 766.
[43] A. Rousseau, et al., Recurrent herpetic keratitis despite antiviral prophylaxis: a virological and pharmacological study, Antivir. Res. 146 (2017) 205–212.
[44] D. Sibley, D.F.P. Larkin, Update on herpes simplex keratitis management, Eye (Lond.) 34 (12) (2020) 2219–2226.
[45] M.S. Wishart, S. Darougar, N.D. Viswalingam, Recurrent herpes simplex virus ocular infection: epidemiological and clinical features, Br. J. Ophthalmol. 71 (9) (1987) 669–672.
[46] F. Hao, et al., Long-term protective effects of AAV9-mesencephalic astrocyte-derived neurotrophic factor gene transfer in parkinsonian rats, Exp. Neurol. 291 (2017) 120–133.
[47] J.R. Mendell, et al., Five-year extension results of the phase 1 START trial of onasemnogene abeparvovec in spinal muscular atrophy, JAMA Neurol. 78 (7) (2021) 834–841.
[48] X. Wang, et al., IL-37bΔ1-45 suppresses the migration and invasion of endometrial cancer cells by targeting the Rac1/NF-κB/MMP2 signal pathway, Lab. Investig. 101 (6) (2021) 760–774.